AGU ADVANCING EARTH AND SPACE SCIENCES

Geophysical Research Letters

RESEARCH LETTER
10.1029/2025GL121404

Drivers of Basal Melt Variability for Pine Island Glacier Ice Shelf: Ocean Forcing Versus Geometric Feedback

Katie Lowery[1,2], **Paul R. Holland**[1], **Pierre Dutrieux**[1], **Anna E. Hogg**[2], and **Noel Gourmelen**[3]

[1]British Antarctic Survey, Cambridge, UK, [2]School of Earth and Environment, University of Leeds, Leeds, UK, [3]School of Geosciences, University of Edinburgh, Edinburgh, UK

Key Points:

- Ocean model simulations reveal how oceanographic forcing and ice shelf geometry changes impact the basal melt rates of Pine Island Glacier
- Ocean variability drives 82% of change in melt whereas geometric changes only drive 8% of change between 2011 and 2021
- Through the reconfiguration of circulation, geometric changes impact the spatial distribution of melt, important for ice-shelf buttressing

Supporting Information:

Supporting Information may be found in the online version of this article.

Correspondence to:

K. Lowery,
katlow20@bas.ac.uk

Citation:

Lowery, K., Holland, P. R., Dutrieux, P., Hogg, A. E., & Gourmelen, N. (2026). Drivers of basal melt variability for Pine Island Glacier Ice Shelf: Ocean forcing versus geometric feedback. *Geophysical Research Letters*, *53*, e2025GL121404. https://doi.org/10.1029/2025GL121404

Received 18 DEC 2025
Accepted 14 MAY 2026

Author Contributions:

Conceptualization: Katie Lowery, Paul R. Holland, Pierre Dutrieux
Formal analysis: Katie Lowery, Paul R. Holland
Investigation: Katie Lowery, Paul R. Holland, Pierre Dutrieux, Anna E. Hogg, Noel Gourmelen
Methodology: Katie Lowery, Paul R. Holland, Pierre Dutrieux, Noel Gourmelen
Project administration: Katie Lowery, Pierre Dutrieux, Anna E. Hogg
Supervision: Paul R. Holland, Pierre Dutrieux, Anna E. Hogg, Noel Gourmelen
Writing – original draft: Katie Lowery

Abstract Since the 1970s, Pine Island Glacier has exhibited thinning, acceleration, and retreat. During the last decade, the ice shelf has undergone major geometric changes, whilst the quantity and temperature of modified Circumpolar Deep Water on the Amundsen Sea continental shelf fluctuated significantly. Untangling how these factors modulate ice-shelf basal melt rates is critical, as ocean-driven melt may be mitigated through emission reductions, whereas geometry-driven retreat may be irreversible. We use ocean model experiments to partition the relative importance of ice geometry and ocean temperature changes in driving melt variability between 2011 and 2021. Simulations use observed ice-shelf geometries from CryoSat-2 and ocean boundary conditions from moorings in Pine Island Bay. Temporal variability of melt and implied ice loss during this period was largely controlled by ocean conditions, while geometric evolution primarily controlled the spatial distribution of melt through cavity circulation reconfiguration, with a non-negligible impact on buttressing.

Plain Language Summary Pine Island Glacier in West Antarctica has contributed more to global sea level rise than any other Antarctic glacier. This ice loss is driven by warm ocean water melting the floating part of the glacier from below. Recent evidence has shown that geometric changes to a glacier can significantly increase ocean melting. If these geometric changes become more important than ocean temperature in driving ocean melting, ice loss could continue even without further ocean warming. In this study, we simulate the ocean-driven melting of Pine Island Glacier between 2011 and 2021, a period marked by large changes in ocean temperature as well as glacier thinning and retreat. We find that changes in ocean melting and implied ice loss were mainly controlled by ocean conditions during this time and geometric changes had minimal impact. This implies that future melting of Pine Island Glacier is likely to depend strongly on ocean temperature. As a result, reducing greenhouse gas emissions can still play an important role in limiting future ice loss and sea-level rise from this glacier.

1. Introduction

The West Antarctic Ice Sheet (WAIS) has been losing mass at an increasing rate (Shepherd et al., 2019), and to date has contributed approximately 6.9 mm to global sea level rise (Otosaka et al., 2023; Rignot et al., 2019). However, future mass loss of the WAIS remains a major uncertainty in future projections of sea level rise (Arias et al., 2021). Much of the observed mass loss has been concentrated in the Amundsen Sea, where widespread thinning, acceleration and grounding line retreat of glaciers has been observed (Adusumilli et al., 2020; Milillo et al., 2022; Mouginot et al., 2014; Rignot et al., 2014; Wingham et al., 2009). Pine Island Glacier (PIG) has lost more mass than any other Antarctic glacier (Rignot et al., 2019), following rapid thinning (Lowery et al., 2025a; Wingham et al., 2009) and acceleration (Joughin et al., 2021; Mouginot et al., 2014; Sun & Gudmundsson, 2023). While its ice speed and discharge have continued to increase in recent years, this mass loss has been offset by increases in snowfall into the drainage basin from atmospheric river extreme weather events (Davison et al., 2023).

Changes in the flow of relatively warm Circumpolar Deep Water (CDW) onto the continental shelf, which melts the base of ice shelves, has contributed to recent dynamic changes (Jacobs et al., 2011, 2012; Jenkins et al., 2010, 2018). Both natural and anthropogenic climatic trends may have contributed to increasing ocean heat content on the continental shelf (Holland et al., 2019, 2022; Naughten et al., 2022), but the observed variability is large and the record is too short to discern significant trends (Dutrieux et al., 2014; Jenkins et al., 2016, 2018). Ice shelf basal melt rates have been shown to scale quadratically with ocean temperatures and increased melt leads to ice acceleration and increased mass loss (Jenkins et al., 2018). However, observed short transient cool periods have

Writing – review & editing: Paul R. Holland, Pierre Dutrieux, Anna E. Hogg, Noel Gourmelen

had limited impact on the ice shelf's velocity (Christianson et al., 2016; Dutrieux et al., 2014; Mouginot et al., 2014).

In addition to climatic drivers, feedbacks linked to ice-shelf cavity geometry strongly influence ice-shelf mass loss by modulating melt rates through their control over how efficiently ocean heat reaches the ice base (Bradley et al., 2022; De Rydt et al., 2014; De Rydt & Naughten, 2024; Holland et al., 2023). De Rydt and Naughten (2024) showed that geometric changes alone can alter melt rates by up to ±75% over two centuries on Amundsen Sea ice shelves, while Holland et al. (2023) found that grounding-line retreat of Thwaites Glacier enhanced melting by 30% between 2011 and 2022. Under PIG, a seabed ridge restricts the access of deep CDW to the inner cavity (Bradley et al., 2022; De Rydt et al., 2014; Dutrieux et al., 2014), making mid-depth waters particularly important for ice shelf melt rates (Dutrieux et al., 2014). Finally, Bradley et al. (2022) showed that a retreat of PIG's calving front inland of the ridge could increase inner cavity basal melt rates by 10%.

These oceanographic and geometric processes evolve simultaneously and non-linearly, complicating efforts to decouple their individual effects. This is a problem because untangling these influences has an important practical consequence. If geometric feedbacks have a strong influence on melting, future ice loss could be self-sustaining and potentially out of control (Arthern & Williams, 2017; Bett et al., 2024; De Rydt & Naughten, 2024). If melt rates are controlled by ocean forcing, anthropogenic climate change and emissions mitigation will play a role in future mass loss. Understanding where and when each of these factors becomes the dominant player in ice shelf melt is critical for accurately predicting future sea level rise.

Previous studies investigating the relative influence of ocean forcing and geometric changes have been limited by sparse observations, often relying on idealized ocean forcing and/or geometry (e.g., Bradley et al., 2022; De Rydt et al., 2014; Dutrieux et al., 2014; Holland et al., 2023; Little et al., 2009). Here, we use the MITgcm ocean model to simulate annual PIG ice shelf melt rates from 2011 to 2021 using observed, time-evolving ice geometry and ocean boundary conditions. This approach allows us to quantify the relative roles of changing ice-shelf geometry and ocean forcing in driving interannual melt-rate variability on PIG.

2. Methods

2.1. Model Setup

To examine detailed patterns of melt rate change, we use an MITgcm model domain covering the PIG ice shelf cavity and a small section of Pine Island Bay (Figure 1a). The configuration follows Holland et al. (2023), who performed related experiments on neighboring Thwaites Glacier using idealized ocean forcing. We used the hydrostatic implementation of MITgcm with a 200 m horizontal and 10 m vertical resolution. Ocean forcing is applied through restoring temperature and salinity conditions on all ocean boundaries. Neither ocean surface fluxes nor a sea ice model are applied. Simulations run for 6 months with a 30 s time step; results are averaged over the final month once an approximate steady state is reached. We apply the standard three-equations ice shelf melt parametrization, directly adopting parameter values from Jenkins et al. (2010), implemented as virtual heat and salt fluxes to maintain constant sea surface height. Constant viscosities (1 m/s^2 horizontal and 5×10^{-4} m/s^2 vertical) and diffusivities (0.1 m^2/s horizontal and 5×10^{-5} m^2/s vertical) are applied, and no subglacial discharge is included. Further model details are provided in Text S1 in Supporting Information S1.

2.2. Ice Shelf Geometry

Ice shelf geometries are derived from the European Space Agency's CryoSat-2 radar altimeter satellite by Lowery et al. (2025a), assuming the July Digital Elevation Model (DEM) represents the annual geometry. Ice shelf draft is calculated by hydrostatic inversion (Figure 1b). Within two ice thicknesses of the grounding line, where the hydrostatic assumption breaks down, the depth of the ice shelf base is linearly interpolated. The grounding line in each simulation is defined where the hydrostatic ice draft depth is below the seabed. All simulations use BedMachine seabed geometry (Morlighem, 2022), modified to match observations from Dutrieux et al. (2014) (Figure 1a). Over the observing period, PIG's ice shelf has thinned by an average of 5 m/yr (Lowery et al., 2025a), its calving front has retreated by 19 km (Joughin et al., 2021) and a central pinning point ungrounded, advecting thick ice downstream (Joughin et al., 2016; Lowery et al., 2025a). The grounding line remained largely stable but shows early signs of retreat in narrow bands (Rignot et al., 2026).

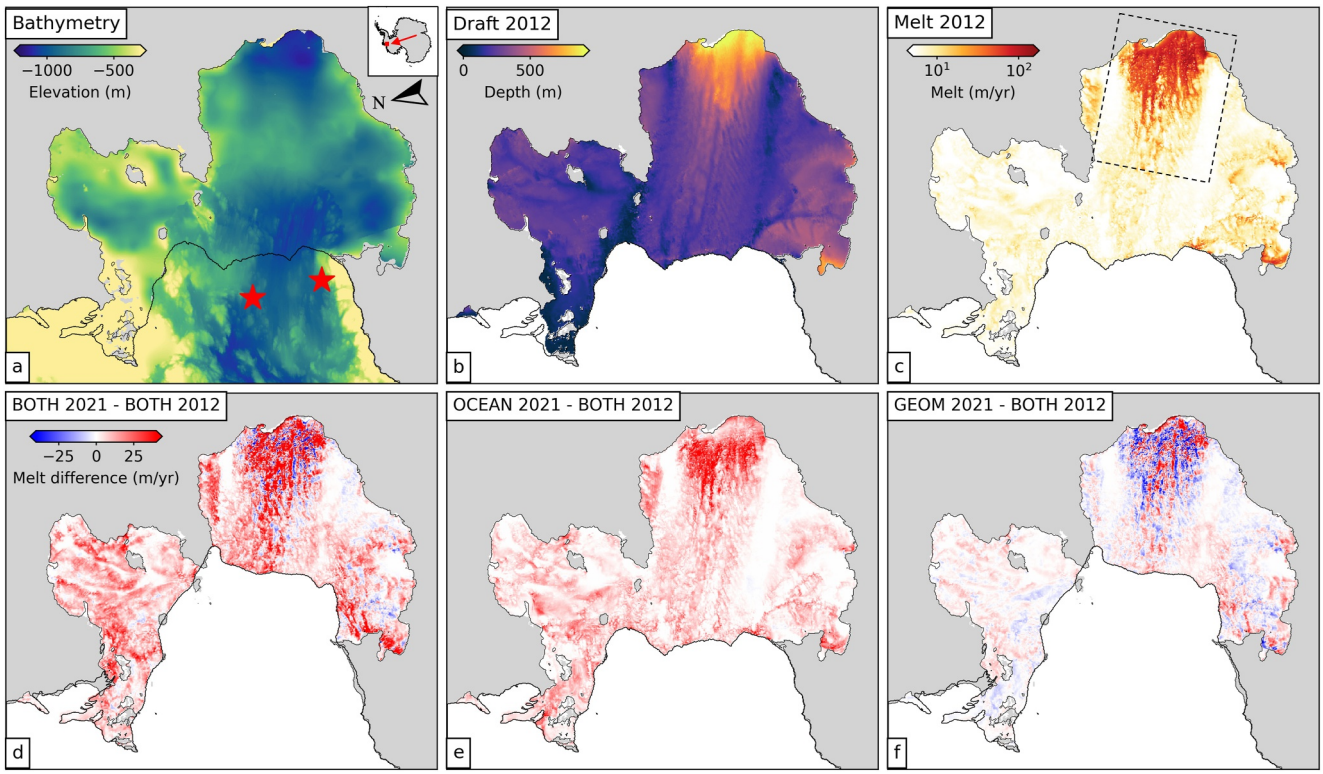

Figure 1. (a) Model domain, showing the adapted BedMachine (Morlighem, 2022) bathymetry used in the model. The red stars indicate ocean mooring locations. (b) 2012 ice shelf draft. (c) Modeled melt in the BOTH 2012 run. (d–f) Difference in melt between the 2021 BOTH, OCEAN 2021, and GEOM 2021 with the BOTH 2021 run, respectively.

2.3. Ocean Forcing

We have used observations from two ocean moorings in Pine Island Bay (red stars in Figure 1a) to create ocean boundary conditions for the model runs (Zhou et al., 2025). The construction of the boundary condition temperature and salinity fields, including the combination and vertical extension of the mooring data, is described in detail in the Text S2 in Supporting Information S1. Our modeling period includes the coldest year on record (2012) but doesn't capture the warmest year (2009), which is outside the observational period for our geometry data set. Ocean forcing profiles are shown in Figure S1 in Supporting Information S1.

2.4. Ice Shelf Buttressing

To further assess the dynamical impact of the spatio-temporal distribution of melt on buttressed land ice, we have used a melt sensitivity data set that maps how melting changes influence the upstream ice-sheet volume above floatation (VAF). Although similar to commonly used buttressing flux response numbers (BFRN), these sensitivities are derived from a single adjoint simulation using automatic differentiation to compute the gradient of grounding-line flux with respect to melt, rather than from multiple forward perturbation experiments (Morlighem et al., 2021; Reese et al., 2018). We use STREAMICE generated fields from Gourmelen et al. (2025), updated from Morlighem et al. (2021), and interpolate them onto our model grid.

2.5. Model Experiments

To separately quantify the effects of ice-shelf geometry and ocean conditions on melting, we conducted three sets of 12 simulations (2011–2021). The first set (BOTH) changes both ocean conditions and ice-shelf geometry each year, representing the most realistic response to changing conditions. The second set (OCEAN) isolates the impact of varying ocean conditions by using annually-varying ocean forcings but retaining the 2012 ice-shelf geometry. The third set (GEOM) isolates the effect of changing ice-shelf geometry by using annually-varying ice geometries but retaining the 2012 ocean boundary conditions. Throughout the analysis, we focus

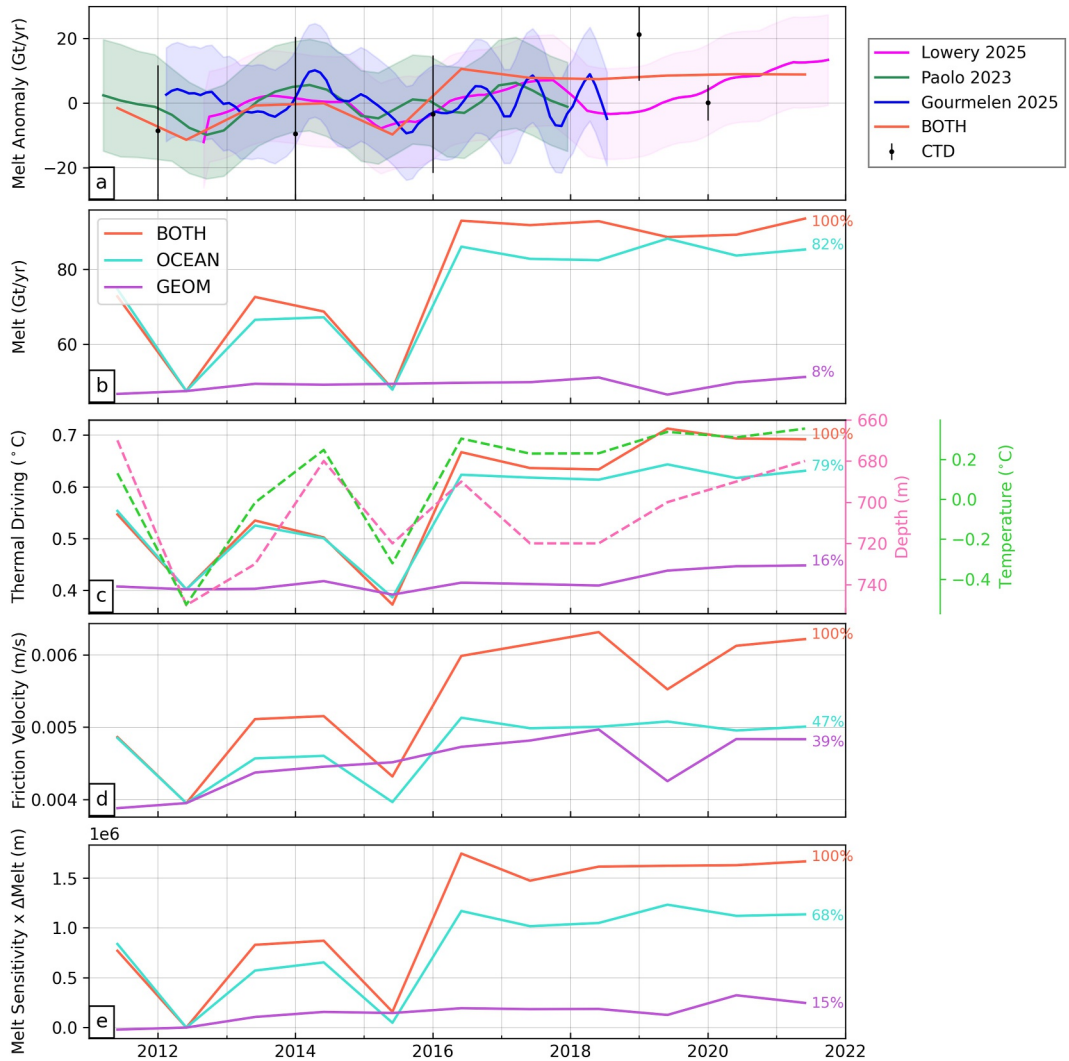

Figure 2. Time series of (a) melt anomalies for the BOTH run and satellite and ocean derived estimates of melt over the area of the ice shelf's main trunk observed by all data sets (black rectangle in Figure 1c), (b) ice shelf integrated melt rates, (c) boundary layer thermal driving, (d) boundary layer friction velocity and (e) the expected total change in Volume above Floatation (VAF) for the given melt rates. (c) Also shows the depth of the 0.8°C isotherm and the average temperature between 450 and 650 m as observed from the ocean moorings. The numbers on the right hand side show the percentage of the change between the 2012 and 2021 BOTH run captured in the corresponding set of runs.

particularly on the 2012 and 2021 runs, the coldest and warmest years, which also provide reasonable bounds for the maximum extent of geometric change during the study period.

3. Results

Ice-shelf integrated melt rate in the BOTH 2012 experiment totals 47 Gt/yr (Figure 2b), consistent with ocean-derived observations (Dutrieux et al., 2014) and satellite estimates (Gourmelen et al., 2025; Lowery et al., 2025a; Paolo et al., 2023) (Figure S2 in Supporting Information S1). We focus primarily on melt anomalies when comparing with satellite products to assess temporal variability. The model reproduces both the pattern and magnitude of variability seen in satellite records (Figure 2a). Melt rates exceed >100 m/yr near the grounding zone and are further structured by basal channels. Lower melt occurs in the northern and southern embayments, while near-zero melt is simulated along the two shear margins (Figure 1c).

3.1. Temporal Variability of Basal Melt

In this section we examine drivers of temporal variability in ice shelf-integrated basal melt (Figure 2). In the BOTH experiment, melt rates increases 97% from 47 in 2012 to 93 Gt/yr in 2021. The first five years show large variability, including the lowest melt rates in 2012 and 2015, whereas after 2016 the time series stabilizes around 90 Gt/yr (Figure 2b). Over the period 2012–2021, the OCEAN simulations reproduced 82% of the increase and are strongly correlated with BOTH ($r = 0.98$), whereas GEOM explains only 8% of the increase and show a weak correlation ($r = 0.41$). The remaining 10% reflects non-linear interactions. This indicates that variability in the ocean conditions dominates changes in basal melt during this period, with geometric evolution playing a secondary role.

In the three-equation parameterization, melt variability arises from changes in ocean temperature near the ice (thermal driving) or in sub–ice shelf currents (friction velocity) (Text S1 in Supporting Information S1). In our simulations, thermal driving variability is controlled by ocean forcing (Figure 2c), while friction velocity reflects both ocean variability and a trend toward stronger currents linked to geometric evolution (Figure 2d). Consistent with De Rydt et al. (2014), variability in average mid-depth (450–650 m) boundary temperatures explains most of the OCEAN melt variability ($r^2 = 0.83$), whereas the depth of the 0.8°C thermocline, indicative of CDW volume, explains little ($r^2 = 0.19$) (Figure 2c).

3.2. Spatial Distribution of Basal Melt

Despite the ocean conditions governing the temporal variability of ice shelf basal melt, the spatial distribution of melt within individual simulations is heavily influenced by the ice shelf geometry (Figures 1d–1f). Under warmer ocean conditions, melt rates increase in a manner that closely preserves the original spatial distribution of melt, resulting in an approximately uniform percentage increase across the main trunk of the ice shelf (Figure 1e and Figure S5b in Supporting Information S1). This is driven by a proportionately uniform warming of the ice-ocean boundary layer (Figure 3g). In contrast, the melt distribution change associated with geometric changes displays large, spatially heterogeneous variations (Figure 1f) which are primarily driven by friction velocity changes associated with the local ice base slope (Figure 3h). While these changes are significant in some regions, they largely cancel out when integrated across the ice shelf, resulting in near zero net change in ice shelf integrated melt (Figure 2b).

3.3. Ice Shelf Cavity Circulation

To understand the changes in boundary layer properties that control modeled basal melt rates, we must examine the ice shelf cavity circulation and its connection to the open ocean. Hereafter, the cavity inshore of the seabed ridge is referred to as the "inner cavity" and the cavity offshore of the ridge as the "outer cavity." In the BOTH 2012 simulation, the inner cavity hosts a strong cyclonic gyre, with a maximum barotropic (depth-averaged) flow of 0.28 Sv. This gyre consists of two smaller subgyres separated by a zone of thicker ice along the glacier's central trunk, which thins the water column, restricting flow between the subgyres to 0.13 Sv (contours in Figure 3a). The strongest inflow of water from the outer cavity into the inner cavity occurs on the southwestern side of the ridge (Figure 3q).

By 2021, cavity temperatures increased by over 1°C (Figures 3i and 3j). Inner-cavity circulation strengthened, with maximum barotropic flow increasing 31% to 0.37 Sv and flow between the two subgyres increasing 72% to 0.23 Sv (Figures 3b and 3n). The dominant inflow across the ridge shifted to the northern ice-shelf side (Figure 3r), driven by increases in both the barotropic and baroclinic components. This raised the total mass flux across the ridge by 55%.

A comparison with the 2021 OCEAN and GEOM simulations shows that most cavity warming in the BOTH 2021 run is driven by ocean boundary conditions (Figure 3k), though geometric changes also cause a small increase in cavity temperatures (Figure 3l). In contrast, circulation strengthening in BOTH 2021 is closely reproduced in GEOM 2021 (22% increase in maximum barotropic flow; 51% increase in connectivity), whereas enhanced melt and freshening of the inner cavity in OCEAN 2021 do not drive a comparable spin-up. The time series of maximum barotropic flow in the inner cavity correlates strongly between BOTH and GEOM ($r = 0.88$) but weakly with OCEAN ($r = 0.38$), indicating this variability is largely driven by increased water-column thickness along the glacier's central trunk (Figure 3). We also note that the increased connectivity of the inner cavity

10.1029/2025GL121404

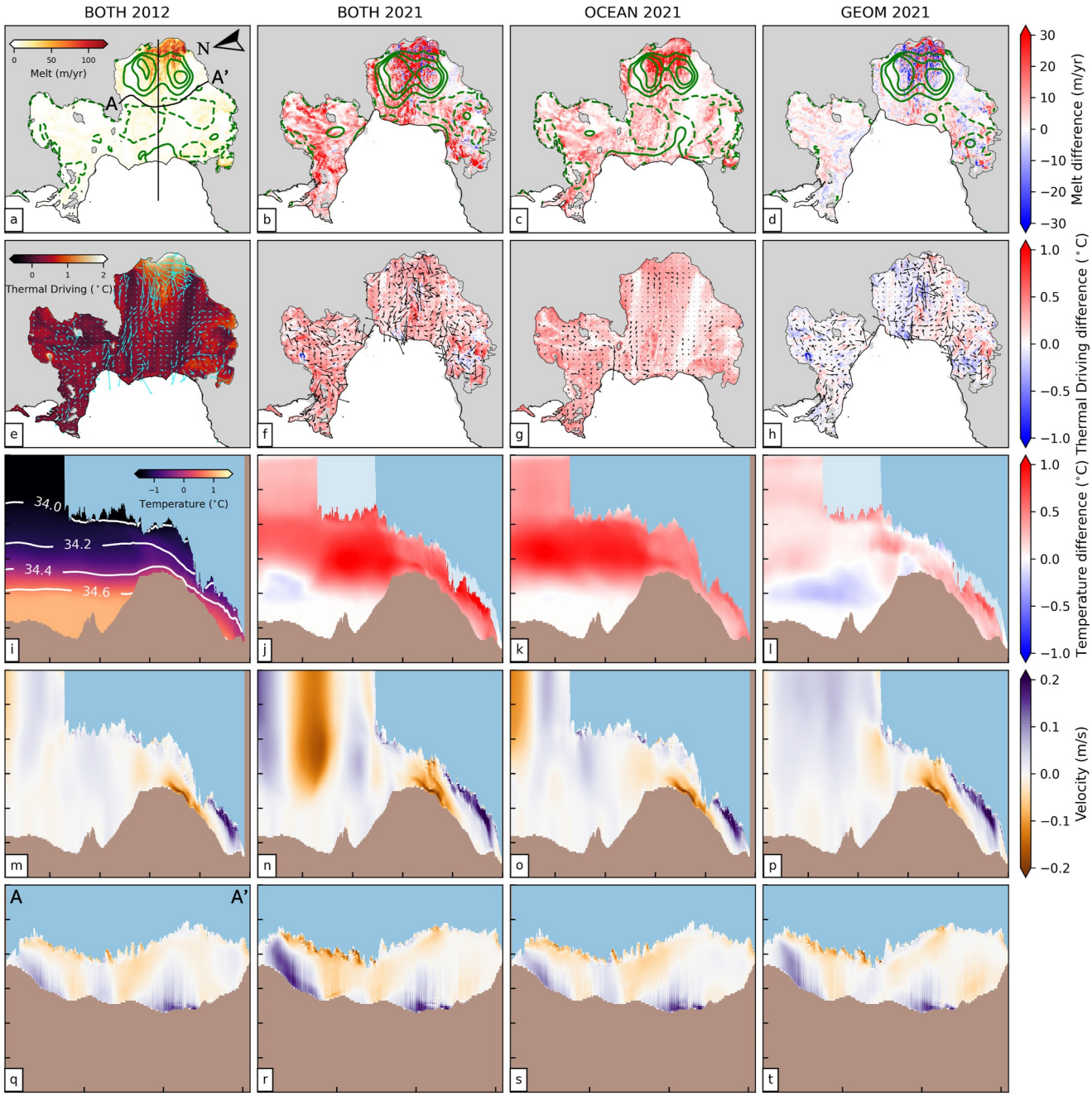

Figure 3. The columns show results from the BOTH 2012, BOTH 2021, OCEAN 2021 and GEOM 2021 runs, respectively. (a) Shows the melt rate map in the BOTH 2012 run, (b–d) show the melt rate difference between that column's run and (a). (a–d) Are all overlaid with barotropic stream function contours in green for that column's run. The contours are separated by 0.75 Sv, starting at 0 (dashed). The second row (e–h) shows the thermal driving and sub-ice currents that drive the friction velocity. (e) Shows the BOTH 2012 run and (f–h) show the differences from (e). The third row (i–l) shows the temperature on the along-glacier-flow black transect in (a). (i) Shows the BOTH 2012 run and (j–l) show the differences from (i). The two shadings of blue ice show the extent of the ice shelf in the two runs. The fourth row (m–p) is the velocity across the same transect for each run, where positive values are out of the page. The final row (q–t) shows velocities across the along seabed ridge transect in (a), where positive values are into the page, toward the grounding line. In (i–t), the *y*-axis ticks mark 200 m depth intervals and the *x*-axis ticks are at 20 km intervals.

circulation in the GEOM 2021 run likely contributes to the clear North-South split in thermal driving change (Figure 3h). Overall, this analysis shows that a large warm anomaly in cavity temperature drives the increased melt in the OCEAN runs whereas the large circulation spin up in the GEOM runs does not change the overall melt rates.

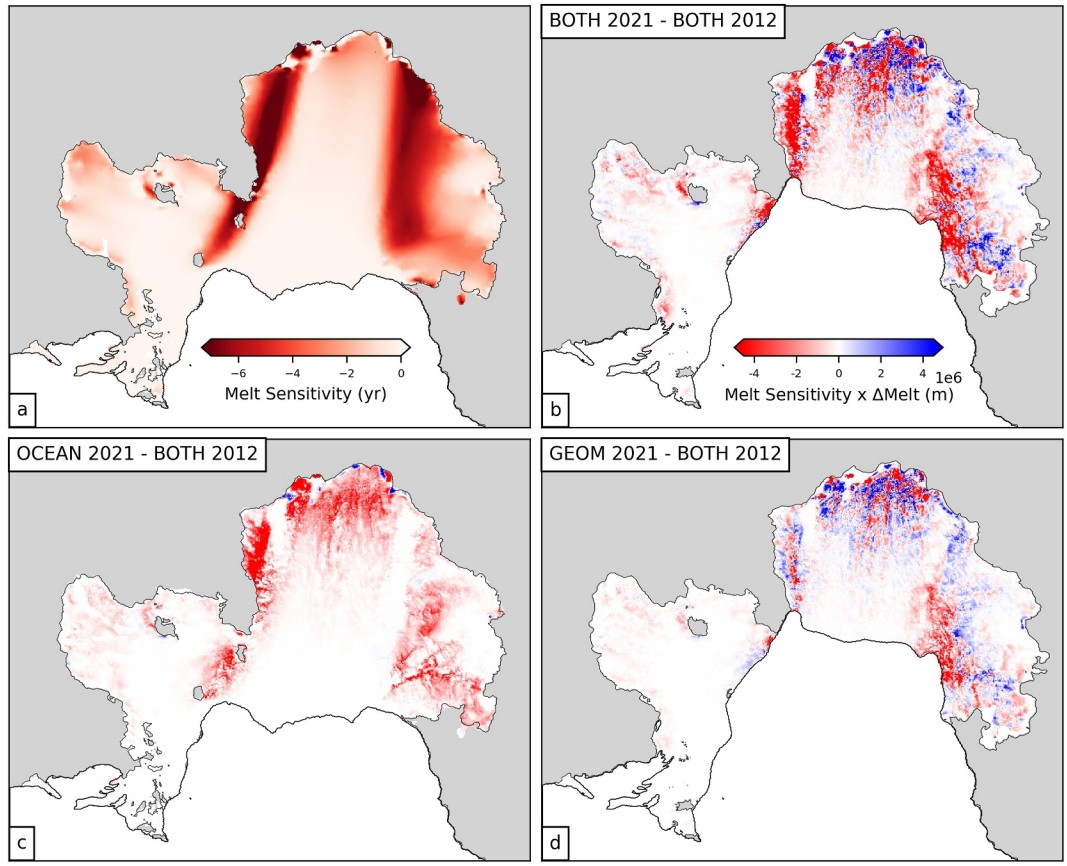

Figure 4. (a) Volume above floatation (VAF) sensitivity to melt from Gourmelen et al. (2025). The units are VAF change (m^3) per melt rate (m/yr) per area (m^2). (b–d) are the melt sensitivity multiplied by the difference in melt between the BOTH 2021, OCEAN 2021, and GEOM 2021 with the BOTH 2012 run, respectively.

3.4. Impact on Ice Shelf Buttressing Capacity

So far we have presented our results in terms of freshwater flux and basal mass balance. However, these metrics do not capture the dynamical consequences of basal melting on upstream grounded ice. An alternative perspective considers how spatial patterns of melt affect the ice shelf's ability to restrain grounded ice flow, which is highly sensitive to basal melt in key regions such as the grounding zone, shear margins, and around pinning points (Morlighem et al., 2021; Naughten et al., 2023; Reese et al., 2018). Because of this spatial variability, not all melt contributes equally to buttressing loss. Here we examine how modeled spatial melt patterns affect the ice shelf's ability to restrain grounded ice flow.

Figure 4a shows PIG's Volume Above Flotation (VAF) sensitivity to melt presented by Gourmelen et al. (2025), where more negative values indicate greater grounded ice loss for a given local melt increase. Shear margins dominate the sensitivity, with smaller contributions from the grounding zone, consistent with other sensitivity fields (Morlighem et al., 2021; Naughten et al., 2023). However, as these are estimates of the linear sensitivity to a perturbation of a single simulation, they likely underestimate grounding zone contributions, which would manifest through nonlinear changes associated with grounding-line retreat.

To estimate expected VAF loss, we multiplied the melt sensitivity field by melt differences from BOTH 2012 and integrated over the ice shelf (Figure 2e). OCEAN simulations explain 68% of VAF change in BOTH, indicating that ocean variability is the dominant driver. However, GEOM explains a larger fraction when evaluated in terms of VAF (15%) than for total melt (8%) (Figures 2e and 2b), making geometry-driven melt changes proportionally more important for VAF loss. Similar results were obtained when repeated using melt sensitivity data from Naughten et al. (2023) (Figure S4e in Supporting Information S1).

To identify the regions driving these temporal changes, we assessed the spatial influence of melt changes on VAF by multiplying melt rate differences by the melt sensitivity field (Figures 4b–4d). In the OCEAN simulations, the influence on VAF largely mirrors the spatial melt pattern (Figure 1d). However, despite their high melt sensitivity, the shear margins contribute little because ocean-driven melt changes there are small. In contrast, the GEOM simulations show a more heterogeneous and localized influence. Enhanced melting along the southern shear margin, particularly following calving events, results in a large contribution from this area. This spatial signature is preserved in the BOTH simulations (Figure 4b), even though the integrated time series remains primarily controlled by oceanic forcing (Figure 2e). We next examine the processes driving melt changes in this shear-margin region.

3.5. Shear Margin Ponding

As discussed above, PIG's shear margins have a high melt sensitivity (Figure 4a). However, throughout the runs melting changes within the shear margins depart from the broader patterns of sensitivity (Figures 1e and 1f). This results in the shear margins disappearing when the melt sensitivity is multiplied by the OCEAN induced melt difference and enhances areas of the southern shear margin when multiplied by the GEOM induced melt difference (Figures 4c and 4d). As the shear margins are critical for the buttressing capacity of the ice shelf, understanding the melt dynamics within them is crucial. We propose two related mechanisms to explain these behaviors:

1. Stagnant freshwater ponding. The shear margins are local ice shelf thickness minima and meltwater accumulates and stagnates within them (Figures S5b and S5c in Supporting Information S1). When ocean temperatures rise, the increased meltwater production deeper in the cavity fills these stagnant regions with a thicker layer of fresh, cold water, buffering heat exchange at the boundary and reducing melting (Figure S5b in Supporting Information S1).
2. Local geometry and pond damming. For stagnant meltwater to persist, thicker downstream ice is needed to act as a dam, trapping the water from being released to the open ocean. In the southern shear margin, calving events over the study period remove this downstream barrier, leading to loss of ponded conditions. As a result, melt increases due to enhanced boundary layer velocities once the pond is removed (Figures S5g–S5i in Supporting Information S1).

4. Discussion

Our results show that the ice shelf basal melt of PIG responds weakly to geometric changes between 2011 and 2021 but strongly to ocean variability (8% and 82%, respectively). When weighted by the spatial distribution of VAF sensitivity to melting, the contribution of geometry increases from 8% to 15%, but remains dwarfed by the influence of ocean forcing (68%). We also note that the ocean contribution increased to 81% when different melt sensitivity data was used (Figure S4e in Supporting Information S1). This overall dominance of oceanic control persists despite geometric feedbacks substantially altering the spatial pattern of basal melt and the inner cavity circulation. Furthermore, we note that there are small (10% and 17%) non-linear components to the overall BOTH melt and expected VAF loss.

Ice shelf integrated results across all simulations agree with the previously described quadratic relationship between thermal driving and melt (Holland et al., 2008; Jenkins et al., 2018) (Figure S7c in Supporting Information S1). Although a linear fit describes the relationship well ($r^2 = 0.96$), when constrained through the origin the RMSE increases beyond that of the quadratic fit (Figure S7c in Supporting Information S1). Further support for a non-linear relationship comes from the linear relationships between thermal driving and friction velocity ($r^2 = 0.68$; Figure S7a in Supporting Information S1), and between their product and melt ($r^2 = 0.92$; Figure S7d in Supporting Information S1), which together indicate a higher-order dependence of melt on thermal driving in these simulations.

Our findings suggest that, under its recent configuration, PIG's ice shelf basal melt rate was governed primarily by ocean conditions. However, the dominance of this process is unlikely to be consistent over longer, decadal to centennial timescales, when ocean warming could trigger positive geometric feedbacks (Rosier et al., 2021). Previous studies have shown that even small-scale geometric changes can trigger large increases in ice shelf basal melt rates (Bradley et al., 2022; Holland et al., 2023). For instance, between 2011 and 2022 at Thwaites Glacier,

geometry-driven melt increases matched those expected from a century of extreme anthropogenic ocean change (Holland et al., 2023). The contrast between these two adjacent systems suggests that the strength and timing of ice–ocean feedbacks are highly sensitive to local geometry and to the period of analysis. Understanding where and when these geometric feedbacks become the dominant control on ice shelf stability is critical to accurately predict long-term ice shelf stability.

Previous studies have investigated the cavity circulation beneath the PIG ice shelf to better understand the delivery of warm CDW to the ice base (e.g., Bradley et al., 2022; De Rydt et al., 2014; De Rydt & Naughten, 2024; Dutrieux et al., 2014; Nakayama et al., 2019; Payne et al., 2007). Our results show that recent geometric changes enhanced the connectivity of the inner cavity, strengthened its circulation, warmed the inner cavity, and increased the mass flux over the seabed ridge. Despite these substantial circulation changes, the net melt response remains limited. There are areas on the ice shelf where changes in these variables do result in large changes in melt rates (Figure 1f), but the area integral of these changes largely cancels out. Consequently, it is possible to identify localized areas where geometric changes have driven larger temporal variability in melt, for example, the Piglet Glacier ice shelf (Figure S6 and Text S3 in Supporting Information S1). Importantly, our findings do not imply that comparable geometric or circulation changes elsewhere, or at other times, would necessarily yield similarly limited melt responses.

PIG's shear margins are critical for its overall buttressing capacity (Morlighem et al., 2021; Naughten et al., 2023). Our simulations suggest that large oceanic changes alone have limited impact on basal melt in these locations, likely due to the ponding of fresh, cold water beneath the shear margins. However, calving disrupts this cold water retention, increasing shear margin melt rates in our GEOM simulations, consistent with results in Bradley et al. (2022). This mechanism is analogous to processes occurring beneath shear margins on Larsen C Ice Shelf, where freezing occurs due to the pooling of cold meltwater in basal hollows (Holland et al., 2009). While freshwater pooling in ice draft minima is not a new idea, this is, to our knowledge, the first suggestion of such a process in warm-cavity shear margins.

This study has several limitations. Firstly, the model domain used is focussed solely on PIG and so has a restoring ocean boundary relatively close to the ice shelf calving front. This introduces lateral density gradients in the open ocean, creating a gyre circulation in front of the ice shelf. Although this circulation is structurally similar to that observed in Pine Island Bay (Thurnherr et al., 2014), here it is driven by the imposed density gradient at the model boundary whereas it is wind/sea-ice driven in the real world. Changes in this gyre structure do not affect the circulation within the cavity, which remains consistent across all runs (Figure 3). Secondly, the melt sensitivity data came from a single adjoint run assuming linear responses to geometry changes, neglecting non-linear and spatially coupled feedbacks. It is unlikely that a method incorporating all responses would produce qualitatively different conclusions, as the areas of high sensitivity remain consistent when a larger perturbation is applied to the adjoint run (Morlighem et al., 2021). These fields are sensitive to the grounding line location in the ice sheet model used to create them. To avoid introducing false sensitivities, we did not interpolate these fields to newly ungrounded areas. This potentially neglects some VAF sensitivity within the GEOM simulations, though as the grounding line migration is small during this time, this does not qualitatively change the conclusions.

Despite these acknowledged limitations, our findings suggest that under its recent configuration, PIG's basal melt variability is primarily driven by ocean temperature conditions, with weaker sensitivity to geometric feedbacks. We note that over this relatively short period the ocean forcing exhibits variability rather than a clear trend, whereas the geometric changes likely reflect an ongoing trend. Nevertheless, we use the variability in both as a proxy for how future trends may influence melt. If the ocean changes considered here are broadly representative of those expected under anthropogenic climate warming, our results suggest that reducing greenhouse gas emissions and limiting ocean warming will still have a dominant influence on PIG's melt rates. These results reinforce the urgent need for climate policy implementation to limit anthropogenic climate warming (Naughten et al., 2023). However, this conclusion hinges on the current configuration of PIG's geometry. The strong variability in geometry-driven feedback mechanisms reported across different glaciers and time scales highlight the need for ongoing high-resolution observations and modeling to understand where and when such feedbacks may become dominant and/or self-sustaining.

5. Conclusions

In this study we have presented results from MITgcm ocean model runs designed to investigate the relative importance of changing ocean conditions and ice shelf geometry on PIG's ice shelf basal melt rates, and how this changes when the sensitivity of grounded ice loss to basal melting is considered. We have shown that the integrated basal melt rate is largely controlled by ocean conditions, and that this is also true for the implied ice loss. When only considering geometric changes, 8% of total melt rates were captured and up to 15% of the resulting implied ice loss. However, we found that geometric changes were the primary control of the spatial distribution of basal melt rates within these simulations, and caused a spin-up of the inner cavity circulation and connectivity. Our results also highlight an important mechanism of freshwater ponding within PIG's shear margins, which acts to prevent warm ocean waters melting these critical areas. The contrast of these results with the nearby Thwaites Glacier suggests variable thresholds for which ocean or geometric changes become the dominant driver of ice shelf basal melt rate variability. The dominance of ocean conditions in driving the melt variability in these simulations highlights the continued control of anthropogenic climate warming on the future of PIG.

Conflict of Interest

The authors declare no conflicts of interest relevant to this study.

Availability Statement

The model outputs can be found via (Lowery et al., 2025b), the model setup can be found via (Lowery et al., 2025c) and the CryoSat-2 DEMs can be found via (Lowery et al., 2025a).

Acknowledgments

This work was led by Katie Lowery at the British Antarctic Survey (BAS) and the School of Earth and Environment at The University of Leeds. Katie Lowery was supported by the Natural Environment Research Council (NERC) Satellite Data in Environmental Science (SENSE) Centre for Doctoral Training (Grant NE/T00939X/1). This research was supported by OCEAN ICE, which is co-funded by the European Union, Horizon Europe Funding Programme for research and innovation under Grant agreement Nr. 101060452 and by UK Research and Innovation. OCEAN ICE Contribution number X. The authors gratefully acknowledge the European Space Agency for the acquisition of CryoSat-2 satellite data. A. E. H and N. G. are supported by ESA through the 5D Antarctica project (4000146702/24/I-KE).

References

Adusumilli, S., Fricker, H. A., Medley, B., Padman, L., & Siegfried, M. R. (2020). Interannual variations in meltwater input to the Southern ocean from Antarctic ice shelves. *Nature Geoscience*, *13*(9), 616–620. https://doi.org/10.1038/s41561-020-0616-z

Arias, P., Bellouin, N., Coppola, E., Jones, R., Krinner, G., Marotzke, J., et al. (2021). Climate change 2021: The physical science basis. Contribution of working group i to the sixth assessment report of the intergovernmental panel on climate change. technical summary. https://doi.org/10.1017/9781009157896.002

Arthern, R. J., & Williams, C. R. (2017). The sensitivity of west Antarctica to the submarine melting feedback. *Geophysical Research Letters*, *44*(5), 2352–2359. https://doi.org/10.1002/2017GL072514

Bett, D. T., Bradley, A. T., Williams, C. R., Holland, P. R., Arthern, R. J., & Goldberg, D. N. (2024). Coupled ice–ocean interactions during future retreat of west antarctic ice streams in the Amundsen Sea sector. *The Cryosphere*, *18*(6), 2653–2675. https://doi.org/10.5194/tc-18-2653-2024

Bradley, A. T., Bett, D. T., Dutrieux, P., De Rydt, J., & Holland, P. R. (2022). The influence of pine island ice shelf calving on basal melting. *Journal of Geophysical Research: Oceans*, *127*(9), e2022JC018621. https://doi.org/10.1029/2022JC018621

Christianson, K., Bushuk, M., Dutrieux, P., Parizek, B. R., Joughin, I. R., Alley, R. B., et al. (2016). Sensitivity of pine island glacier to observed ocean forcing. *Geophysical Research Letters*, *43*(20), 10817–10825. https://doi.org/10.1002/2016GL070500

Davison, B. J., Hogg, A. E., Rigby, R., Veldhuijsen, S., van Wessem, J. M., van den Broeke, M. R., et al. (2023). Sea level rise from west antarctic mass loss significantly modified by large snowfall anomalies. *Nature Communications*, *14*(1), 1479. https://doi.org/10.1038/s41467-023-36990-3

De Rydt, J., Holland, P. R., Dutrieux, P., & Jenkins, A. (2014). Geometric and oceanographic controls on melting beneath pine island glacier. *Journal of Geophysical Research: Oceans*, *119*(4), 2420–2438. https://doi.org/10.1002/2013JC009513

De Rydt, J., & Naughten, K. (2024). Geometric amplification and suppression of ice-shelf basal melt in west Antarctica. *The Cryosphere*, *18*(4), 1863–1888. https://doi.org/10.5194/tc-18-1863-2024

Dutrieux, P., De Rydt, J., Jenkins, A., Holland, P. R., Ha, H. K., Lee, S. H., et al. (2014). Strong sensitivity of pine island ice-shelf melting to climatic variability. *Science*, *343*(6167), 174–178. https://doi.org/10.1126/science.1244341

Gourmelen, N., Jakob, L., Holland, P., Dutrieux, P., Goldberg, D., Bevan, S., et al. (2025). The influence of subglacial Lake discharge on Thwaite's glacier ice-shelf melting and grounding-line retreat. *Nature Communications*, *16*(1), 2272. https://doi.org/10.1038/s41467-025-57417-1

Holland, P. R., Bevan, S. L., & Luckman, A. J. (2023). Strong ocean melting feedback during the recent retreat of thwaites glacier. *Geophysical Research Letters*, *50*(8), e2023GL103088. https://doi.org/10.1029/2023GL103088

Holland, P. R., Bracegirdle, T. J., Dutrieux, P., Jenkins, A., & Steig, E. J. (2019). West Antarctic ice loss influenced by internal climate variability and anthropogenic forcing. *Nature Geoscience*, *12*(9), 718–724. https://doi.org/10.1038/s41561-019-0420-9

Holland, P. R., Corr, H. F., Vaughan, D. G., Jenkins, A., & Skvarca, P. (2009). Marine ice in Larsen ice shelf. *Geophysical Research Letters*, *36*(11). https://doi.org/10.1029/2009GL038162

Holland, P. R., Jenkins, A., & Holland, D. M. (2008). The response of ice shelf basal melting to variations in ocean temperature. *Journal of Climate*, *21*(11), 2558–2572. https://doi.org/10.1175/2007JCLI1909.1

Holland, P. R., O'Connor, G. K., Bracegirdle, T. J., Dutrieux, P., Naughten, K. A., Steig, E. J., et al. (2022). Anthropogenic and internal drivers of wind changes over the Amundsen Sea, west Antarctica, during the 20th and 21st centuries. *The Cryosphere*, *16*(12), 5085–5105. https://doi.org/10.5194/tc-16-5085-2022

Jacobs, S. S., Jenkins, A., Giulivi, C. F., & Dutrieux, P. (2011). Stronger ocean circulation and increased melting under pine island glacier ice shelf. *Nature Geoscience*, *4*(8), 519–523. https://doi.org/10.1038/ngeo1188

Jacobs, S. S., Jenkins, A., Hellmer, H., Giulivi, C. F., Nitsche, F., Huber, B., & Guerrero, R. (2012). The Amundsen Sea and the Antarctic ice sheet. *Oceanography*, *25*(3), 154–163. https://doi.org/10.5670/oceanog.2012.90

Jenkins, A., Dutrieux, P., Jacobs, S., Steig, E. J., Gudmundsson, G. H., Smith, J., & Heywood, K. J. (2016). Decadal ocean forcing and antarctic ice sheet response: Lessons from the Amundsen Sea. *Oceanography*, *29*(4), 106–117. https://doi.org/10.5670/oceanog.2016.103

Jenkins, A., Dutrieux, P., Jacobs, S. S., McPhail, S. D., Perrett, J. R., Webb, A. T., & White, D. (2010). Observations beneath pine island glacier in west Antarctica and implications for its retreat. *Nature Geoscience*, *3*(7), 468–472. https://doi.org/10.1038/ngeo890

Jenkins, A., Shoosmith, D., Dutrieux, P., Jacobs, S., Kim, T. W., Lee, S. H., et al. (2018). West antarctic ice sheet retreat in the Amundsen Sea driven by decadal Oceanic variability. *Nature Geoscience*, *11*(10), 733–738. https://doi.org/10.1038/s41561-018-0207-4

Joughin, I., Shapero, D., Smith, B., Dutrieux, P., & Barham, M. (2021). Ice-shelf retreat drives recent pine island glacier speedup. *Science Advances*, *7*(24), eabg3080. https://doi.org/10.1126/sciadv.abg3080

Joughin, I., Shean, D. E., Smith, B. E., & Dutrieux, P. (2016). Grounding line variability and subglacial Lake drainage on pine island glacier, Antarctica. *Geophysical Research Letters*, *43*(17), 9093–9102. https://doi.org/10.1002/2016GL070259

Little, C. M., Gnanadesikan, A., & Oppenheimer, M. (2009). How ice shelf morphology controls basal melting. *Journal of Geophysical Research*, *114*(C12). https://doi.org/10.1029/2008JC005197

Lowery, K., Dutrieux, P., Holland, P. R., Hogg, A. E., & Gourmelen, N. (2025b). Mitgcm model outputs for the ocean in pine island Bay between 2011 and 2021 (version 1.0). [Dataset]. https://doi.org/10.5285/cbc6eb20-de95-457d-9000-c78b0ae9ee51

Lowery, K., Dutrieux, P., Holland, P. R., Hogg, A. E., Gourmelen, N., & Wallis, B. J. (2025a). Spatio-temporal melt and basal channel evolution on pine island glacier ice shelf from cryosat-2. *The Cryosphere*, *19*(10), 4893–4911. https://doi.org/10.5194/tc-19-4893-2025

Lowery, K., Holland, P. R., & Dutrieux, P. (2025c). Model setup for simulations of melting beneath pine island glacier ice shelf.

Milillo, P., Rignot, E., Rizzoli, P., Scheuchl, B., Mouginot, J., Bueso-Bello, J. L., et al. (2022). Rapid glacier retreat rates observed in west Antarctica. *Nature Geoscience*, *15*(1), 48–53. https://doi.org/10.1038/s41561-021-00877-z

Morlighem, M. (2022). *Measures bedmachine Antarctica, version 3*. NASA National Snow and Ice Data Center Distributed Active Archive Center. https://doi.org/10.5067/FPSU0V1MWUB6

Morlighem, M., Goldberg, D., Dias dos Santos, T., Lee, J., & Sagebaum, M. (2021). Mapping the sensitivity of the Amundsen Sea embayment to changes in external forcings using automatic differentiation. *Geophysical Research Letters*, *48*(23), e2021GL095440. https://doi.org/10.1029/2021GL095440

Mouginot, J., Rignot, E., & Scheuchl, B. (2014). Sustained increase in ice discharge from the Amundsen Sea embayment, west Antarctica, from 1973 to 2013. *Geophysical Research Letters*, *41*(5), 1576–1584. https://doi.org/10.1002/2013GL059069

Nakayama, Y., Manucharyan, G., Zhang, H., Dutrieux, P., Torres, H. S., Klein, P., et al. (2019). Pathways of ocean heat towards pine island and thwaites grounding lines. *Scientific Reports*, *9*(1), 16649. https://doi.org/10.1038/s41598-019-53190-6

Naughten, K. A., Holland, P. R., & De Rydt, J. (2023). Unavoidable future increase in west antarctic ice-shelf melting over the twenty-first century. *Nature Climate Change*, *13*(11), 1222–1228. https://doi.org/10.1038/s41558-023-01818-x

Naughten, K. A., Holland, P. R., Dutrieux, P., Kimura, S., Bett, D. T., & Jenkins, A. (2022). Simulated twentieth-century ocean warming in the Amundsen Sea, west Antarctica. *Geophysical Research Letters*, *49*(5), e2021GL094566. https://doi.org/10.1029/2021GL094566

Otosaka, I. N., Shepherd, A., Ivins, E. R., Schlegel, N.-J., Amory, C., van den Broeke, M. R., et al. (2023). Mass balance of the Greenland and Antarctic ice sheets from 1992 to 2020. *Earth System Science Data*, *15*(4), 1597–1616. https://doi.org/10.5194/essd-15-1597-2023

Paolo, F. S., Gardner, A. S., Greene, C. A., Nilsson, J., Schodlok, M. P., Schlegel, N.-J., & Fricker, H. A. (2023). Widespread slowdown in thinning rates of west Antarctic ice shelves. *The Cryosphere*, *17*(8), 3409–3433. https://doi.org/10.5194/tc-17-3409-2023

Payne, A. J., Holland, P. R., Shepherd, A. P., Rutt, I. C., Jenkins, A., & Joughin, I. (2007). Numerical modeling of ocean-ice interactions under pine island bay's ice shelf. *Journal of Geophysical Research*, *112*(C10). https://doi.org/10.1029/2006jc003733

Reese, R., Gudmundsson, G. H., Levermann, A., & Winkelmann, R. (2018). The far reach of ice-shelf thinning in Antarctica. *Nature Climate Change*, *8*(1), 53–57. https://doi.org/10.1038/s41558-017-0020-x

Rignot, E., Mouginot, J., Morlighem, M., Seroussi, H., & Scheuchl, B. (2014). Widespread, rapid grounding line retreat of pine island, Thwaite's, smith, and Kohler glaciers, west Antarctica, from 1992 to 2011. *Geophysical Research Letters*, *41*(10), 3502–3509. https://doi.org/10.1002/2014GL060140

Rignot, E., Mouginot, J., Scheuchl, B., van den Broeke, M., van Wessem, M. J., & Morlighem, M. (2019). Four decades of Antarctic ice sheet mass balance from 1979–2017. *Proceedings of the National Academy of Sciences*, *116*(4), 1095–1103. https://doi.org/10.1073/pnas.1812883116

Rignot, E., Scheuchl, B., Barre, J. B., Brancato, V., Charrier, L., Chen, H., et al. (2026). Thirty years of glacier grounding line retreat in Antarctica. *Proceedings of the National Academy of Sciences*, *123*(10), e2524380123. https://doi.org/10.1073/pnas.2524380123

Rosier, S. H. R., Reese, R., Donges, J. F., De Rydt, J., Gudmundsson, G. H., & Winkelmann, R. (2021). The tipping points and early warning indicators for pine island glacier, west Antarctica. *The Cryosphere*, *15*(3), 1501–1516. https://doi.org/10.5194/tc-15-1501-2021

Shepherd, A., Gilbert, L., Muir, A. S., Konrad, H., McMillan, M., Slater, T., et al. (2019). Trends in Antarctic ice sheet elevation and mass. *Geophysical Research Letters*, *46*(14), 8174–8183. https://doi.org/10.1029/2019GL082182

Sun, S., & Gudmundsson, G. H. (2023). The speedup of pine island ice shelf between 2017 and 2020: Revaluating the importance of ice damage. *Journal of Glaciology*, *69*(278), 1983–1991. https://doi.org/10.1017/jog.2023.76

Thurnherr, A. M., Jacobs, S. S., Dutrieux, P., & Giulivi, C. F. (2014). Export and circulation of ice cavity water in pine island Bay, west Antarctica. *Journal of Geophysical Research: Oceans*, *119*(3), 1754–1764. https://doi.org/10.1002/2013JC009307

Wingham, D. J., Wallis, D. W., & Shepherd, A. (2009). Spatial and temporal evolution of pine island glacier thinning, 1995–2006. *Geophysical Research Letters*, *36*(17). https://doi.org/10.1029/2009GL039126

Zhou, S., Dutrieux, P., Giulivi, C. F., Jenkins, A., Silvano, A., Auckland, C., et al. (2025). The ocean ice mooring compilation: A standardised, pan-Antarctic database of ocean hydrography and current time series. *Earth System Science Data Discussions*, *2025*(10), 1–20. https://doi.org/10.5194/essd-17-5693-2025